PERFORMANCE OF AN ACOUSTO-OPTIC BRAGG CELL UNDER ION MICROBEAM IRRADIATION

Alan H. Paxton, Harald Schone, Edward W. Taylor, Stanley McKinney
US Air Force Phillips Laboratory/VTMC; Kirtland AFB, NM 87117-5776

B. L. Doyle
Sandia National Laboratories MS 1056
Albuquerque, NM 87185-1056

1. ABSTRACT

An acousto optic (AO) deflector composed of $PbMoO_4$ was exposed to 4 MeV protons while operating under Bragg angle conditions. An ion beam in air of 1 mm width was directed normal to the crystal face and laser beam. Between exposures, the approximately 13 mm $\times$ 8.5 mm AO deflector was mechanically translated in two dimensions in front of the fixed ion beam. The AO diffraction efficiency was mapped and was observed to change as a function of ion beam location and dose rate. These effects are attributed to the induced change in the temperature distribution of the crystal, which changed the sonic velocity and refractive index. Similar effects were observed when the ion beam was directed at the acoustic transducer.

2. INTRODUCTION

The application of photonics technologies in radiation environments is receiving increased attention. Radiation induced effects in acousto-optic (AO) devices operating under Bragg conditions have been reported. These effects include transient changes to: attenuation, bandwidth, diffraction efficiency, deflection angle, and polarization states of the output beams; see Ref. 1 and papers cited therein. The focus of this paper is to report on the exposure of an AO Bragg cell to an ion microbeam source. While various AO Bragg devices composed of TeO_2, InP, GaP, and LiNbO3 have been investigated using an ion microbeam, only the responses induced in $PbMoO_4$ are reported here. These responses were observed to closely parallel those observed earlier using broad area sources as well as a CO_2 laser to simulate radiation-induced thermal effects[2].

3. EXTERNAL ION BEAM ANALYSIS

Proton exposure of a $PbMoO_4$ acousto-optic (AO) device was performed at the Sandia nuclear microbeam facility. Sandia's microprobe can deliver ions ranging from protons up to gold ions with energies ranging from 1 MeV to 60 MeV. The available ion beam spot sizes are about 1μm or less in vacuum and about 50 to 100μm in air depending on beam intensity and ion species. The laser, the light detector, and the AO device were mounted on a single plate to minimize misalignment due to size changes of supports with temperature and due to vibration. This also allowed the plate to be moved to change the point of incidence of the microbeam on the AO crystal, so that optical alignment was maintained. The test arrangement required too large a space to fit almost any, if not

any, existing microbeam vacuum chamber. Sandia has developed an external microbeam analysis setup, that can be used to test samples as large as 30 cm x 30 cm. The ion beam is energy analyzed and collimated before entering a magnetic quadrupole lens with a 3.5 mm bore. The beam is focused onto the sample through a thin (15μm) mylar or Al air-to-vacuum window at the end of the chamber. The ion beam current was measured by replacing the sample with a Faraday cup. Additionally, the number of ion-induced secondary electrons emitted from the vacuum side of the window were recorded, and the beam current on the target was monitored by the electron count rate. The AO modulator exposures were performed using 4.0 MeV protons focused to approximately 1mm and with intensities of about 90 nA. To minimize the X-rays produced by the ion beam traversing the air gap, a distance of less than 2mm between the sample and the vacuum window was chosen. The X-ray radiation background during a typical proton irradiation was below 0.3mrad/hr. A 2D map of the device response to the beam radiation as function of beam position on the modulator surface was produced by translating the AO device, together with the entire test setup, in front of the ion beam.

4. EXPERIMENT

The AO device that we exposed was a $PbMoO_4$ Isomet 1206C-1 modulator, used with a 1233A1 RF oscillator. It was operated at 110 MHz, at RF power level of 0.925W. The power levels of the deflected and undeflected output light beams were monitored during the H^+ exposure. The experimental setup is shown in Fig. 1. The crystal of the AO device was exposed in a grid of spots with 2.0 mm spacing in both the horizontal (z) and vertical (y) dimensions. The microbeam was stopped within 100 μm of the crystal surface, so the temporary degradation of the AO performance was due to thermal effects, since charge creation and crystal defect generation did not take place in the region traversed by the laser beam. The exposure time was typically 40 s, and the performance was monitored for 15 s after the microbeam was cut off by the Faraday cup. Performance returned to the pre-exposure conditions within the 15 seconds.

Contour plots of the device diffraction efficiency are shown in Figs. 2 through 4. The y, z coordinate gives the location on the crystal face of the H^+ beam during exposure. Our definition of diffraction efficiency is

$$\eta = \frac{p_1}{p_1 + p_0'}, \tag{1}$$

where p_1 is the power of the deflected optical beam, and p_0' is the optical output power in the direction of the incident beam. The H^+ beam was unblocked at time $t = 0$, so Fig. 2 gives the unperturbed diffraction efficiency, and the contours are an indication of the experimental error. Figures 3 and 4 show the diffraction efficiency as a function of the microbeam location at t=10 s and t=40 s. There was no significant change from the distribution from t=30 s (not shown) to t=40 s, so the crystal temperature distribution had reached steady state by this time. The laser beam was located 3.2±0.4 mm from the transducer, and 1.0±0.2 mm from the irradiated crystal face.

Very little degradation of the diffraction efficiency occurred for H^+ locations that were not between the laser beam and the transducer, as is seen in Figs 3 and 4. Another notable feature

is the occurrence of the highest diffraction efficiency for beam locations that are centered in the z-dimension. This effect is explained by the theoretical discussion in the next section.

5. DISCUSSION OF RESULTS

To understand the thermal effects caused by the microbeam, we numerically calculated C_d, the coefficient for diffraction of power from the incident light wave into the diffracted wave[3] for a number of values of z with y=2.5 mm. To do this, first we obtained the equilibrium temperature increase in the crystal due to the microbeam by solving Laplace's equation. Boundary conditions corresponded to constant temperature at the heatsink and a derivative proportional to the beam energy flux at the crystal surface. Heat loss due to radiation and convection was estimated to be less than 1% of the incident power, and these loss mechanisms were ignored. The aberration of the acoustic wave at its intersection with the optical beam was obtained from the temperature distribution, and it was expanded as a spectrum of plane waves. The optical beam only satisfied the condition for Bragg diffraction for the portion of the spectrum very near zero spatial frequency. Therefore C_d was proportional to the square of the zero-frequency component of the acoustic wave.[4]

When the energy deposition on the crystal was centered at $z = 0$, there was no tilt component to the acoustic wave, and the main lobe of the spatial frequency spectrum was centereded at zero. For decentered deposition, the acoustic wave had a tilt component which served to detune it from Bragg resonance with the optical wave. This caused a greater decrease in C_d than did the higher order aberrations.[3] To obtain the overall diffraction efficiency from C_d, a coupled wave equation would have to be applied, but a consideration of the magnitude of C_d is sufficient to understand the "W" shape of the diffraction efficiency curve.

6. ACKNOWLEDGEMENT

This work was sponsored by the Defense Nuclear Agency under DNA MIPR# 96-2006 and Work Unit 52223.

7. REFERENCES

1. E. W. Taylor, S. P. Chapman, M. A. Kelly, A. D. Sanchez, J. Stohs, E. Kinsley, and D. M. Craig, Conf. on Photonics for Space Environments III, San Diego, CA, 1995, Proc. SPIE 2482 (1995) 16.

2. E. W. Taylor and M. A. Kelly, Conf. on Photonics for Space Environments III, San Diego, CA, 1995, Proc. SPIE 2482 (1995) 40.

3. A. H. Paxton and E. W. Taylor, Conf. on Photonics for Space Environments IV, Denver, CO, 1996, Proc. SPIE 2811(1996) 38.

4. M. G. Cohen and E. I. Gordon, Bell System Tech. J. 44 (1965) 693.

FIGURE CAPTIONS

Figure 1. Experimental setup for measuring the performance of an AO cell under H^+ irradiation. The setup, including all the elements shown here except the beam tube, was mounted on an aluminum plate which was bolted to a translation stage that allowed it to be moved relative to the H^+ beam.

Figure 2. Contour plot showing the diffraction efficiency as a function of ion beam location on the crystal. The transducer is at location y=0, and the light beam enters the crystal at the face at z=6.5. The plot is for time t=0 s, just before the ion beam was unblocked.

Figure 3. Contour plot showing the diffraction efficiency as a function of ion beam location on the crystal. The transducer is at location y=0. The plot is for time t=10 s, and the ion beam was unblocked at t=0.

Figure 4. Contour plot showing the diffraction efficiency as a function of ion beam location on the crystal. The transducer is at location y=0. The plot is for time t=40 s, and the ion beam was unblocked at t=0.

Figure 5. Comparison of experimental values of diffraction efficiency with a theoretical curve of the efficiency for scattering from the input beam to the diffracted beam. The curves are plotted as a function of the location of the center of the ion beam at the surface of the crystal. The qualitative structure of the two curves is similar. In order to simulate the overall diffraction efficiency, a coupled wave equation would have to be applied to the interaction of the laser beam with the aberrated sound wave.

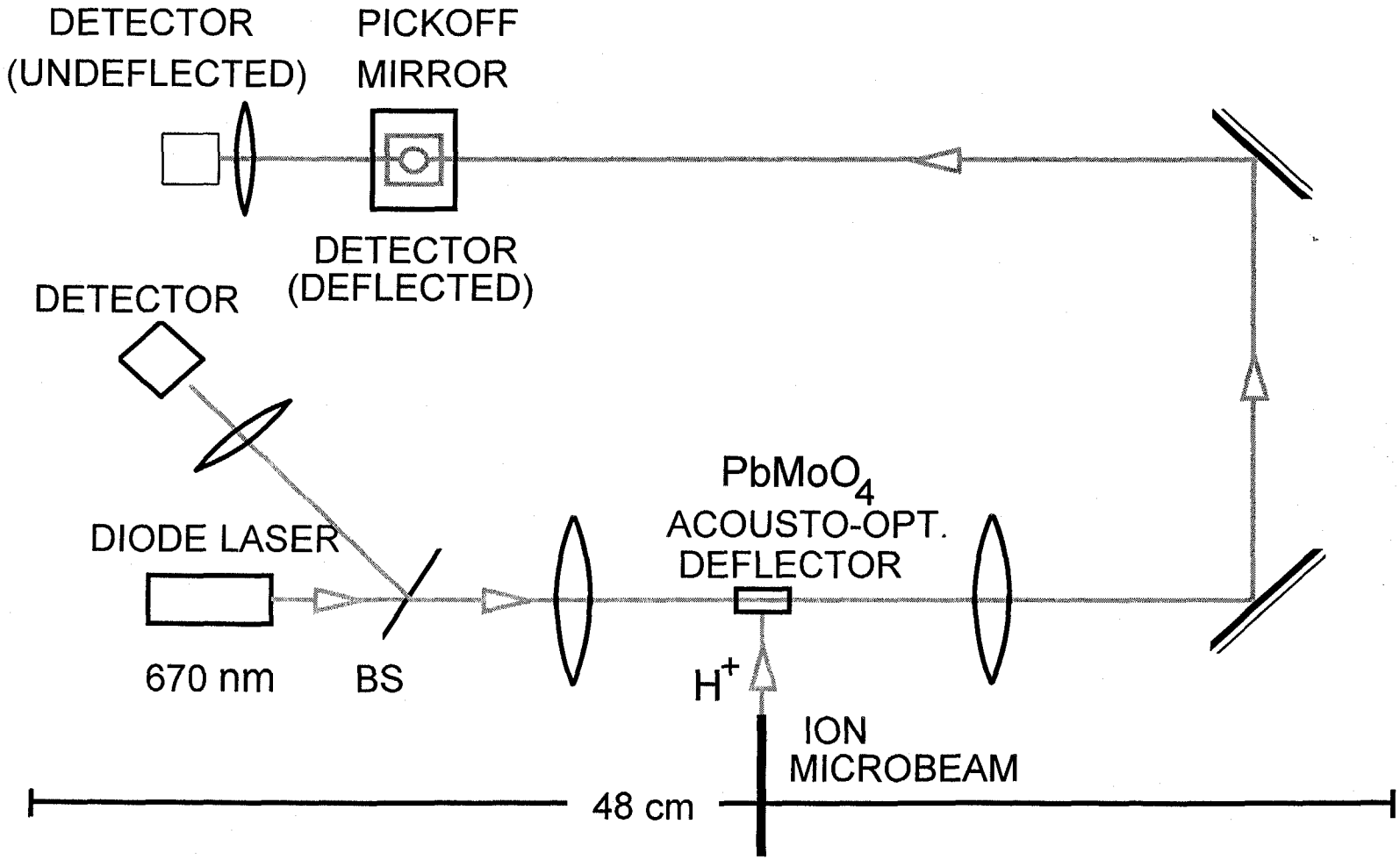
DETECTOR
(UNDEFLECTED)
PICKOFF
MIRROR
DETECTOR
(DEFLECTED)
DETECTOR
DIODE LASER
670 nm
BS
PbMoO4
ACOUSTO-OPT.
DEFLECTOR
H+
ION
MICROBEAM
48 cm

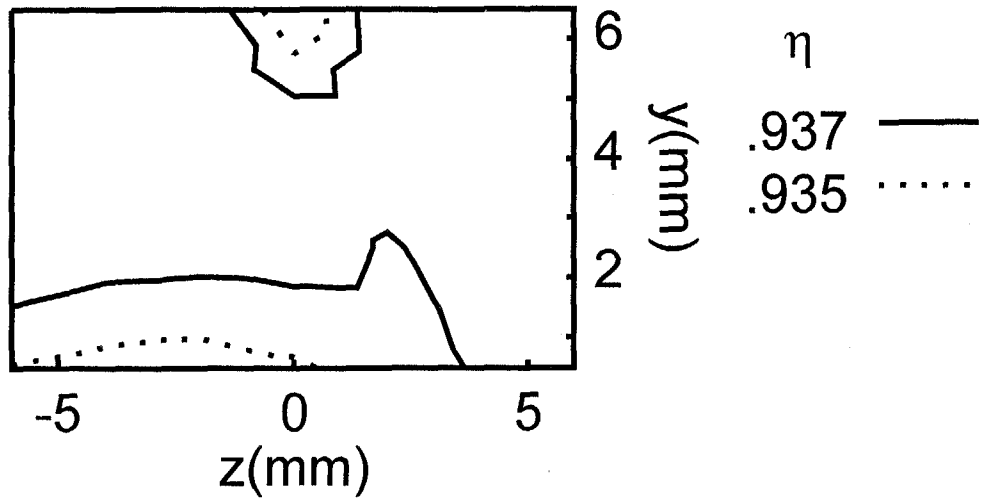
6
4
2
y(mm)
η
.937
.935
-5
0
5
z(mm)

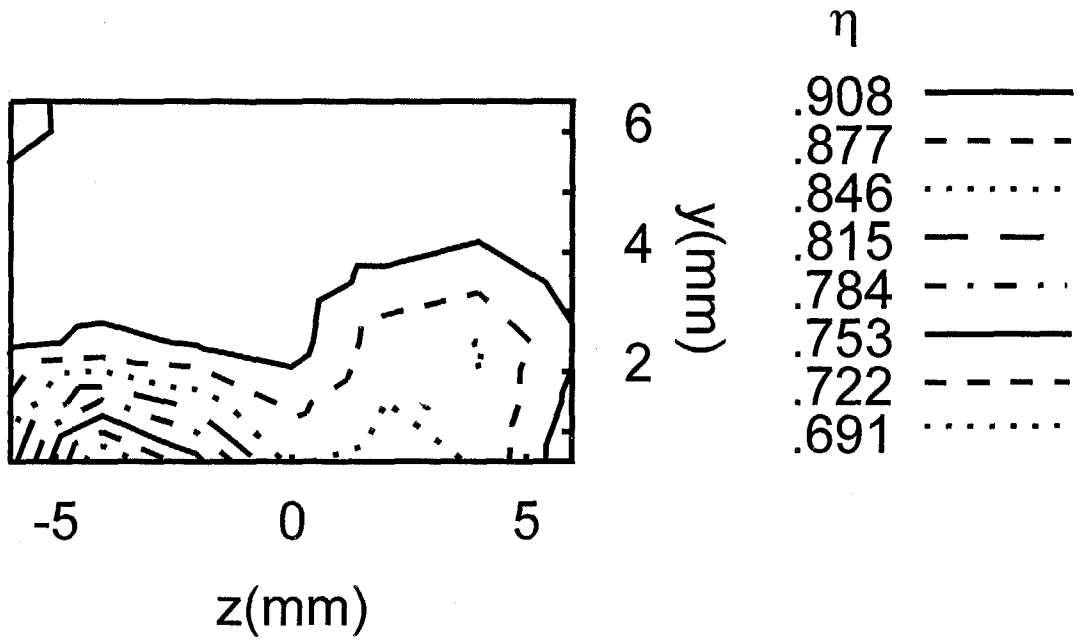
η
.908
.877
.846
.815
.784
.753
.722
.691
6
4
2
y(mm)
-5
0
5
z(mm)

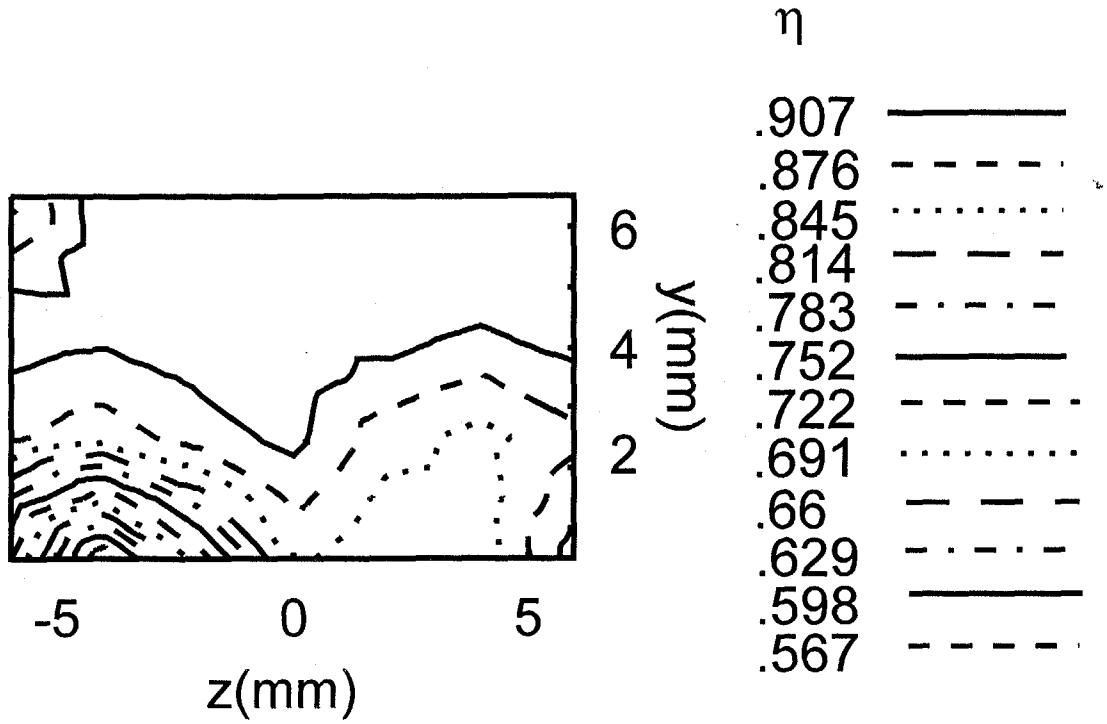
η
.907
.876
.845
.814
.783
.752
.722
.691
.66
.629
.598
.567
6
4
2
y(mm)
-5
0
5
z(mm)

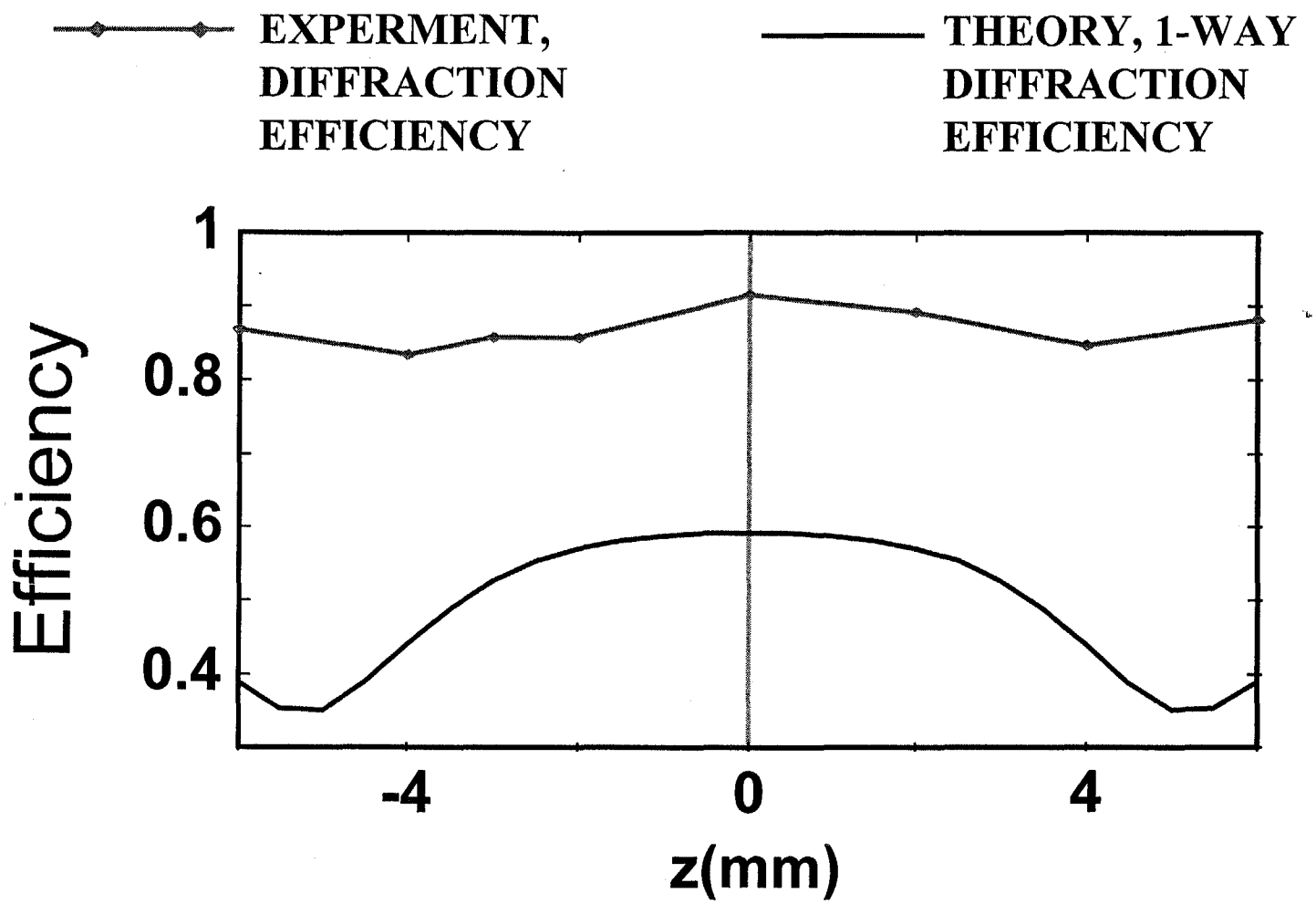
EXPERMENT, DIFFRACTION EFFICIENCY
THEORY, 1-WAY DIFFRACTION EFFICIENCY
Efficiency
1
0.8
0.6
0.4
-4
0
4
z(mm)